

Detectable, defect-free dark photon dark matter

David Cyncynates[✉] and Zachary J. Weiner[✉]

Department of Physics, University of Washington, Seattle, WA 98195, U.S.A.

Ultralight dark photons are compelling dark matter candidates, but their allowed kinetic mixing with the Standard Model photon is severely constrained by requiring that the dark photons do not collapse into a cosmic string network in the early Universe. Direct detection in minimal production scenarios for dark photon dark matter is strongly limited, if not entirely excluded; discovery of sub-meV dark photon dark matter would therefore point to a nonminimal dark sector. We describe a model that evades such constraints, capable of producing cold dark photons in any parameter space accessible to future direct detection experiments. The associated production dynamics yield additional signatures in cosmology and small-scale structure, allowing for possible positive identification of this particular class of production mechanisms.

Evidence for cold dark matter abounds in astrophysical and cosmological observations [1–3], but not for its fundamental nature—the mass and spin of its constituents or its interactions with the visible sector. Dark photons are among the best-motivated candidates for new light degrees of freedom and are common features of grand unified theories and string theory [4–11]. They may constitute all the dark matter in scenarios ranging from minimal gravitational production during inflation [12–16] to non-thermal mechanisms involving additional new degrees of freedom [17–21]. At low energies, a dark photon can interact with the Standard Model (SM) through kinetic mixing with the ordinary photon, yielding signatures in cosmology [22–27], astrophysics [27–39], and the laboratory [28, 40–50]; numerous dark matter haloscopes are poised to probe a vast space of unexplored dark photon masses and kinetic mixing [51–80]. Such theoretical and observational promise demands understanding whether the parameter space within experimental reach also allows for consistent dark photon dark matter production.

Recent work demonstrated a stringent upper bound on the kinetic mixing that allows for viable dark photon dark matter [27]: the dark photon backreacts on the Higgs responsible for its mass and, with large enough couplings at large enough energy density, can restore the dark $U(1)_D$ gauge symmetry. The associated Goldstone boson winds about sites of symmetry restoration, seeding string vortices that deplete the energy in the cold, coherent dark electromagnetic fields. Such a defect network dilutes like radiation and cannot be the dark matter.

The dark gauge coupling g_D , which controls the strength of backreaction of dark gauge bosons onto the Higgs, is a free parameter in all production mechanisms and can simply be tuned small enough to avoid defect formation. But the dark photon’s kinetic mixing with the Standard Model photon ε is generated by heavy fermions charged under both $U(1)_Y$ and $U(1)_D$ and is therefore also proportional to the dark gauge coupling g_D [81]. Fig. 1 shows that, for known production mechanisms, the prospects for probing the kinetic mixing of dark photon dark matter are severely limited, if not entirely absent.

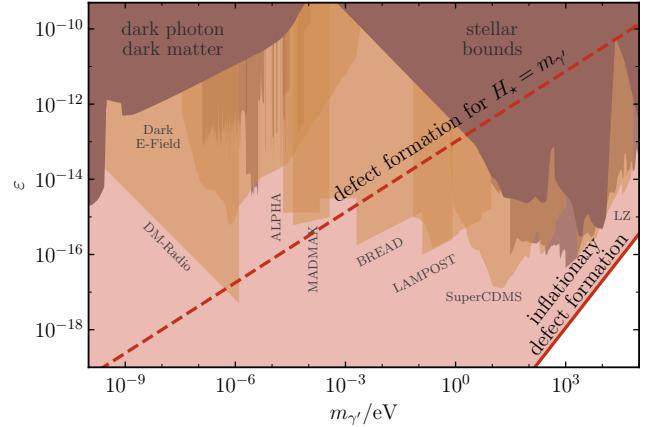


FIG. 1. Dark photon dark matter parameter space, including exclusions from astrophysical [27–38], cosmological [22–27], and haloscope observations [51–74] in gray, and experimental prospects [75–80] in yellow. For inflationary production [12], defect formation with a fiducial kinetic mixing $\varepsilon \sim eg_D/16\pi^2$ [81, 82] excludes the bulk of parameter space [27] (red shaded region). Most other models effectively produce dark photons no later than when the Hubble rate $H_* \approx m_{\gamma'}$, bounding the kinetic mixing to be below the dashed red line.

Direct detection in most parameter space would therefore point to a nonminimal dark sector.

In this letter we describe an extension of the Abelian-Higgs model that realizes cold dark photon dark matter with kinetic mixing detectable by any planned or proposed laboratory experiment. We discuss additional signatures in cosmology and small-scale structure that could corroborate the nonminimality of the model. A companion article [83] explores further generalizations thereof, discusses the implications of defect formation on existing dark photon production mechanisms in detail, and enumerates more *ad hoc* means to generate a hierarchy between the kinetic mixing and the dark gauge coupling.

The Abelian-Higgs theory is described by the La-

grangian¹

$$\mathcal{L}_{\text{AH}} = -\frac{1}{4}F_{\mu\nu}F^{\mu\nu} + \frac{1}{2}D_\mu\Phi(D^\mu\Phi)^* - V_\Phi(\Phi), \quad (1)$$

where A is the dark photon, Φ is the dark Higgs field, $D_\mu = \partial_\mu - ig_D A_\mu$ is the gauge covariant derivative, and the Higgs potential V_Φ is the usual symmetry breaking potential,

$$V_\Phi(\Phi) = \frac{\lambda}{4} \left(|\Phi|^2 - v^2 \right)^2. \quad (2)$$

In the broken phase, the dark photon acquires a mass $m_{\gamma'} = g_D v$ and contributes $g_D^2 |\Phi|^2 A_\mu A^\mu / 2$ to the Higgs's effective potential. If this contribution (which coincides with the dark photon's energy density ρ_A when it is non-relativistic) exceeds λv^4 , then the dark photon backreacts strongly onto the Higgs and seed topological defects. If dark photon dark matter is produced at a Hubble rate H_* , evading defect formation requires²

$$g_D \lesssim 10^{-14} \lambda^{1/4} \left(\frac{m_{\gamma'}}{\mu\text{eV}} \right) \left(\frac{H_*}{\mu\text{eV}} \right)^{-3/8}. \quad (3)$$

In the minimal setup, kinetic mixing is generated by loops of a few heavy fermions with $\mathcal{O}(1)$ charge [81] with $\varepsilon \sim g_D e / 16\pi^2$, so this constraint strongly limits direct detection prospects, as illustrated in Fig. 1. The general considerations leading to Eq. (3) motivate two possible solutions: either modulate the parameters of the Abelian-Higgs theory to raise the threshold for defect formation or delay production as late as possible, such that the dark photon never has enough energy density to exceed the defect formation threshold.

These possibilities may be realized by extending the Abelian-Higgs theory Eq. (1) with couplings to a singlet scalar ϕ as

$$\begin{aligned} \mathcal{L} = & -\frac{W(\phi)}{4}F_{\mu\nu}F^{\mu\nu} + \frac{X(\phi)}{2}D_\mu\Phi(D^\mu\Phi)^* \\ & + Y(\phi)V_\Phi(\Phi) + \frac{1}{2}\partial_\mu\phi\partial^\mu\phi - V(\phi). \end{aligned} \quad (4)$$

We discuss concrete choices of the coupling functions W , X , and Y below. The dark Higgs and photon are made canonical via the rescalings $\Psi = \sqrt{X(\phi)}\Phi$ and $\mathcal{A}_\mu = \sqrt{W(\phi)}A_\mu$. Written in terms of the canonical fields, the Higgs's potential is

$$Y(\phi)V_\Phi(\Phi) = \frac{\lambda Y(\phi)}{4X(\phi)^2} \left(|\Psi|^2 - X(\phi)v^2 \right)^2, \quad (5)$$

¹ We use natural units in which $\hbar = c = 1$ and the reduced Planck mass $M_{\text{pl}} = 1/\sqrt{8\pi G}$, fix a cosmic-time Friedmann-Lemaître-Robertson-Walker (FLRW) metric $ds^2 = dt^2 - a(t)^2 \delta_{ij} dx^i dx^j$ with $a(t)$ the scale factor, and employ the Einstein summation convention for spacetime indices. Dots denote derivatives with respect to cosmic time t , and the Hubble rate is $H \equiv \dot{a}/a$.

² This threshold assumes the dark photon is composed of nonrelativistic modes; we discuss its generalization in Ref. [83].

and its covariant derivative is

$$\sqrt{X(\phi)}D_\mu\Phi = \partial_\mu\Psi - \frac{ig_D\mathcal{A}_\mu\Psi}{\sqrt{W(\phi)}} - \frac{\partial_\mu\sqrt{X(\phi)}}{\sqrt{X(\phi)}}\Psi. \quad (6)$$

The form of Eqs. (5) and (6) motivates absorbing the ϕ dependence of the theory into its fundamental parameters as

$$g_D(\phi) = g_D/\sqrt{W(\phi)}, \quad (7a)$$

$$\lambda(\phi) \equiv \lambda Y(\phi)/X(\phi)^2, \quad (7b)$$

$$v(\phi) \equiv v\sqrt{X(\phi)}. \quad (7c)$$

If the scalar is homogeneous, i.e., $\phi(t, \mathbf{x}) = \bar{\phi}(t)$, then its cosmological evolution permits the theory's parameters to vary over cosmological history.

The threshold for defect formation then depends on the scalar as $\lambda(\phi)v(\phi)^4 = \lambda v^4 Y(\phi)$. One might be tempted to arrange for $Y(\phi) \gg 1$ to simply raise the threshold for defect formation as high as needed. This solution is no different than simply taking large λ in the bare Abelian-Higgs Lagrangian, and it requires the Higgs to be a composite degree of freedom because fundamental Higgs scattering violates perturbative unitarity for $\lambda \gtrsim 4\pi$. Such issues aside, a still more appealing solution would utilize the scalar field's dynamics to not only prevent defect formation but also generate the dark photon relic abundance.

We turn to dynamical mechanisms that evade defect formation by delaying production, illustrated by Fig. 2. In general, the mass sets a kinematic barrier for particle production; resonant production with rolling scalars effectively requires the scalar's mass $m_\phi \gtrsim m_{\gamma'}$ for efficient dark photon production. As the scalar starts rolling when $H \sim m_\phi \gtrsim m_{\gamma'}$, in these scenarios production typically occur no later than $H \sim m_{\gamma'}$. On the other hand, scalar couplings offer a means to suppress the dark photon's mass in the early Universe: via Eq. (7),

$$m_{\gamma'}(\phi) \equiv m_{\gamma'}\sqrt{X(\phi)/W(\phi)}. \quad (8)$$

In such a scenario, $X(\phi)$ and/or $W(\phi)$ must evolve so that the theory's parameters take on their bare values at the present day. However, the scalar couplings generate derivative interactions that cannot necessarily be neglected as ϕ evolves. This feature is precisely what enables production of a relic abundance of dark photons via tachyonic resonance, familiar from other dark photon models [17–20].

In the presence of a homogeneous scalar, the linearized equation of motion for the transverse polarizations of the dark photon \mathcal{A}_\pm is

$$0 = \ddot{\mathcal{A}}_\pm + H\dot{\mathcal{A}}_\pm + \omega_\pm^2\mathcal{A}_\pm, \quad (9)$$

with an effective squared frequency

$$\omega_\pm^2 = \frac{k^2}{a^2} + m_{\gamma'}^2 \frac{\bar{X}}{\bar{W}} - \frac{H}{2} \frac{\dot{\bar{W}}}{\bar{W}} - \frac{\partial_t^2 \sqrt{\bar{W}}}{\sqrt{\bar{W}}} \quad (10)$$

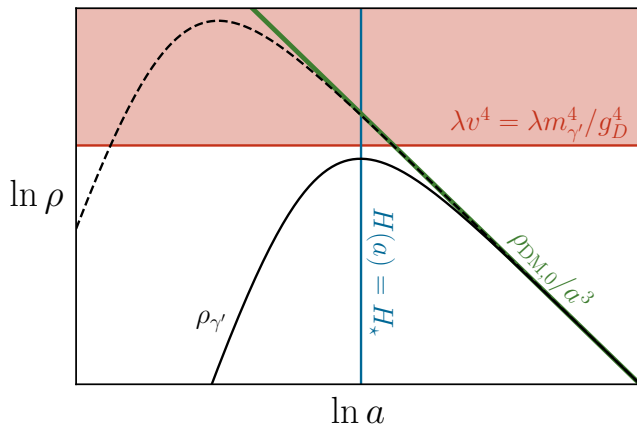


FIG. 2. Illustration of dark photon production that avoids defect formation by delaying the time of production. After it is produced and becomes nonrelativistic, the dark matter has a known energy density at any scale factor a (indicated by the green line) extrapolated from its present-day value. For any choice of model parameters, its energy density would exceed the threshold for defect formation (in the red shaded region) at some early time. By sufficiently delaying the production of dark photons, i.e., until some critical Hubble rate H_* (indicated by the blue line), they never trigger defect formation (per the solid black curve). Dark photons produced too early (as in the dashed black curve) collapse into a string network that is not viable cold dark matter.

[with the shorthand $\bar{W} = W(\bar{\phi})$ and $\bar{X} = X(\bar{\phi})$]. Whenever ω_{\pm}^2 is negative (i.e., due to the coupling terms outweighing the mass and momentum contributions), the transverse dark photon modes grow exponentially. Time derivatives of \bar{W} are necessarily negative in Eq. (10) as \bar{W} decreases from the large values that suppress $m_{\gamma'}$ at early times. Since the transverse modes are derivatively coupled only to the kinetic function $W(\phi)$, we set $X(\phi) = 1$ and $Y(\phi) = 1$ from here on out.³

To illustrate the production mechanism, we present a concrete example and compute the dark photon relic abundance, present the expanded parameter space accessible to direct detection experiments, and discuss other constraints on the model. We consider a so-called runaway potential [84–86] for the scalar where

$$V(\phi) = M^2 f^2 e^{-\phi/f} \equiv m_{\phi}^2 f^2 e^{-(\phi-\phi_0)/f}. \quad (11)$$

The latter equality defines m_{ϕ} as the scalar's effective mass at its homogeneous initial condition $\bar{\phi} = \phi_0$; the scalar remains frozen until $H \approx m_{\phi}$. An approximate solution to the scalar's homogeneous equation of motion,

$$0 = \ddot{\bar{\phi}} + 3H\dot{\bar{\phi}} + V'(\bar{\phi}), \text{ is}$$

$$\bar{\phi}(t) = \phi_0 + f \ln [1 + (m_{\phi} t)^2]. \quad (12)$$

Full solutions exhibit moderate oscillations in $\ln t$ about Eq. (12). Without loss of generality, we take $\phi_0 < 0$ and assume a coupling of the form

$$W(\phi) = 1 + e^{-\beta\phi/f}, \quad (13)$$

constructed such that $W \approx 1$ after ϕ crosses zero, which occurs at $m_{\phi} t_d \approx e^{-\phi_0/2f}$ when the Hubble rate is $H_d = 1/2t_d$.

To compute the abundance of dark photons sourced by the rolling scalar, we may first approximate the solution to Eq. (9) to $\mathcal{O}([k/m_{\phi}]^2)$ as

$$\frac{\mathcal{A}_{\pm}(t, k)}{\mathcal{A}(0, k)} \approx [1 + (m_{\phi} t)^2]^{-\beta/2} [1 + (k/m_{\phi})^2 \delta\mathcal{A}(t)]. \quad (14)$$

Equation (14) solves the $k \rightarrow 0$ limit of Eq. (9) when $\delta\mathcal{A} = 0$; plugging Eq. (14) back into Eq. (9) yields a leading- k correction of

$$\delta\mathcal{A}(t) = \int_0^{m_{\phi} t} dx (1+x^2)^{\beta} {}_2F_1(1/4, \beta, 5/4, -x^2). \quad (15)$$

We set $a = 1$ when $H = m_{\phi}$. Taking $x \gg 1$, the growth rate of the small- k modes scales as $\mathcal{A}_{\pm} \propto (k/m_{\phi})^2 (m_{\phi} t)^{\beta+1/2}$. Amplification continues roughly until any other term in Eq. (9) becomes important, i.e., at

$$t_{\star}(k) \approx \min \left\{ \frac{1}{2H_d} \left(\sqrt{\beta^2 + \frac{\beta}{2} \frac{2H_d}{m_{\gamma'}}} \right)^{\frac{1}{\beta+1}}, \frac{2\beta^2 + \beta}{2k^2/m_{\phi}} \right\}. \quad (16)$$

Modes with larger wave number stop growing earlier, and the power spectrum of \mathcal{A}_{\pm} peaks near

$$\frac{k_{\star}}{m_{\phi}} \approx 2^{\frac{\beta}{2(\beta+1)}} \frac{m_{\gamma'}}{\sqrt{H_d m_{\phi}}} \left(\frac{H_d}{m_{\gamma'}} \sqrt{\beta \left(\beta + \frac{1}{2} \right)} \right)^{\frac{2\beta+1}{2\beta+2}}. \quad (17)$$

As $m_{\gamma'} \gg H_d$ in general, all amplified modes are highly nonrelativistic once $W(\phi) \rightarrow 1$. Provided β is greater than a few, the time of production Eq. (16) reduces to $t_{\star} \approx 1/2H_d$. After this time, the mode amplitude of the nonrelativistic modes decreases as the mass continues to increase $\mathcal{A} \propto W^{1/4}$ per the WKB approximation. Integrating the spectrum of \mathcal{A} over wave number up to k_{\star} to estimate $\rho_A(t_{\star}) \approx m_{\gamma'}^2 \langle \mathcal{A}^2 \rangle$ at production,

$$\frac{\rho_A(t_{\star})}{H_d^4} \equiv \mathcal{N}_{\beta} \left(\frac{m_{\phi}}{H_d} \right)^{2\beta-1} \left(\frac{H_d}{m_{\gamma'}} \right)^{\frac{\beta-5}{\beta+1}}, \quad (18)$$

where the β -dependent coefficient is

$$\mathcal{N}_{\beta} = \frac{(2\beta^2 + \beta)^{\frac{3(3\beta+1)}{2(\beta+1)}} \Gamma(5/4)^2 \Gamma(\beta - 1/4)^2}{3\pi^2 (1+4\beta)^2 2^{\frac{2\beta^2-\beta}{\beta+1} + \frac{7}{2}} \Gamma(\beta)^2}. \quad (19)$$

³ The longitudinal mode has derivative couplings via $X(\phi)$, though efficient production requires that X decreases with time; we discuss this and other possibilities in Ref. [83].

This result reproduces full numerical solutions within one to two orders of magnitude for $-\phi_0/f \gtrsim 5$ [below which the errors are dominated by the approximation made in Eq. (12)]. More detailed exposition is provided in Ref. [83]. Note that the success of the mechanism is not unique to these particular choices of W and V —the salient features are a substantial mass suppression at early times [so that $m_{\gamma'}(\phi_0) \ll m_\phi$] and a coupling function that evolves faster with ϕ than the potential (so that tachyonic resonance is efficient). We discuss other possibilities in Ref. [83].

The relic abundance of dark photon dark matter is

$$\frac{\Omega_{\gamma'}}{\Omega_{\text{DM}}} = \mathcal{N}_\beta \left(\frac{m_\phi}{H_d} \right)^{2\beta-1} \left(\frac{H_d}{m_{\gamma'}} \right)^{\frac{\beta-5}{\beta+1}} \frac{H_d^2}{M_{\text{pl}}^2} \sqrt{\frac{H_d}{H_{\text{eq}}}} \quad (20)$$

where $H_{\text{eq}} \approx 2.2 \times 10^{-28}$ eV is the Hubble rate at matter-radiation equality. Production may occur as late as desired by choosing m_ϕ or ϕ_0 to set t_d . To produce dark photons heavier than the scalar, their initial mass $m_{\gamma'}(\phi_0) \approx m_{\gamma'} e^{\beta\phi_0/2}$ must be smaller than m_ϕ , requiring $\beta\phi_0$ to be sufficiently large (and negative). Achieving the correct relic abundance turns out to place a more stringent requirement of $-\beta\phi_0/f$ in the range of 150 – 250, with a corresponding mass suppression more than enough to produce dark photons with any mass of interest. For cosmology to proceed as observed, the dark matter must exist by, say, a redshift $z \sim 10^6$ or 10^7 , making decoupling at $H_d = 10^{-22}$ eV a useful benchmark. As evinced by Fig. 3, such late production is sufficient for viable dark photon dark matter in reach of any future experiment.

Other resonant production mechanisms (via oscillating pseudoscalars [17–20] or scalars [21]) require the system to reach a regime where the dark photon backreacts on the scalar sourcing it—otherwise, the dark matter would mostly comprise scalars rather than vectors. These nonlinear dynamics can only be understood with 3D simulations, and the energy exchange that occurs at backreaction often results in a rough equipartition between the dark photon and scalar. At attractive feature of scenarios involving runaway scalars is that they become energetically subdominant without relying on nonlinear dynamics. The runaway scalar solution uniquely tracks the background such that its relative abundance is

$$\Omega_\phi(t) \equiv \frac{\rho_\phi(t)}{3H(t)^2 M_{\text{pl}}^2} \approx \left(\frac{2f}{M_{\text{pl}}} \right)^2 \quad (21)$$

in both the radiation- and matter-dominated epochs [90–92]. Comparing to the abundance of the dark photons $\Omega_{\gamma'} = \rho_{\gamma'}/3H^2 M_{\text{pl}}^2$ provides a reasonable proxy to assess whether backreaction is important. At production (when the two decouple), the dark photons have an abundance $\Omega_{\gamma'}(t_\star) \sim [H_{\text{eq}}/H_\star]^{3/2} \sim 10^{-10} [H_\star/10^{-21} \text{ eV}]^{-3/2}$. The scalar’s decay constant need not be anywhere near M_{pl} to arrange for its energy density to well above the dark photon’s.

At large enough f the scalar could have an observable impact on cosmology. In the radiation era, the scalar effectively increases the Hubble rate as small-scale CMB modes enter the horizon, enhancing diffusion damping of the photon-baryon plasma [93–95]. Bounds on extra radiation content from the CMB largely derive from this effect and currently amount to a bound $\Delta N_{\text{eff}}/N_{\text{eff}} \lesssim 5\%$ to 10%.⁴ Current measurements therefore already limit f to be (roughly) below $M_{\text{pl}}/10$, while CMB-S4, which projects sensitivity to $\Delta N_{\text{eff}}/N_{\text{eff}} \sim 1\%$, would probe yet smaller decay constants $f/M_{\text{pl}} \sim 0.03$.

Resonant production mechanisms in general feature dark matter with a density power spectrum sharply peaked at order unity on some characteristic scale. In the case of axion or scalar oscillations, the scalar mass is what sets this characteristic wave number [17–21]. On the other hand, the vector mass sets a kinematic barrier below which resonant enhancement is typically inefficient. The kinetic coupling suppresses the vector mass during production, allowing for peak scales of order m_ϕ which can be far below the present-day dark photon mass.

Density fluctuations at the power spectrum peak collapse shortly after matter-radiation equality, forming dense small scale structure at astrophysically relevant scales [96]. The typical peak wave number is set by the Hubble rate at production [per Eq. (17)], which in the large- β limit corresponds to structures with mass

$$M \sim 2 \times 10^9 M_\odot \left(\frac{\beta}{10} \right)^{-3} \left(\frac{m_\phi}{10^{-22} \text{ eV}} \right)^{-3/2}. \quad (22)$$

That minihalos can be much more massive than expected from the dark photon’s mass itself provides a signature that distinguishes this model from other resonant production mechanisms. While the presence of such massive substructure does not guarantee that the dark photon has kinetic mixing of any particular size, if an experiment measures a kinetic mixing larger than possible for other nonthermal production mechanisms, substructure in the dark matter halo would necessarily be so massive. Figure 3 illustrates the mass-coupling parameter space for which upcoming astrometric [87] and photometric [88, 89] surveys would be able to probe such extremal substructure.

In the class of models we discuss, the kinetic mixing evolves in the early Universe, but there is no reason *a priori* that the evolution must have stopped before the present day. The constant term in Eq. (13), for instance, could itself be promoted to a slow function of ϕ ,

⁴ The scalar is not precisely equivalent to free-streaming neutrinos—genuine constraints would require a proper treatment of the dynamics of its perturbations. In addition, runaway scalars redshift like matter after matter-radiation equality, providing enhanced and distinctive phenomenology compared to pure radiation (which instead becomes energetically subdominant.)

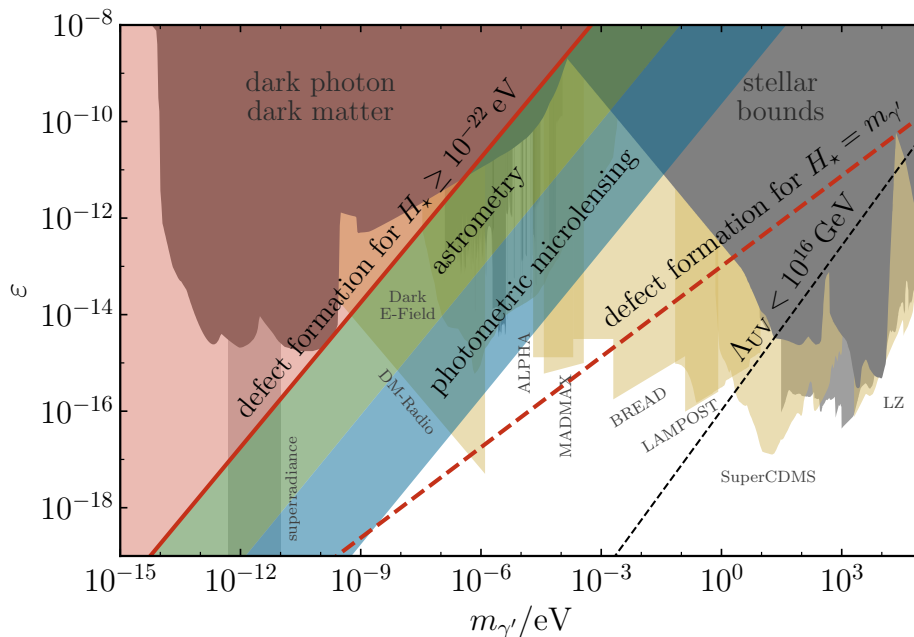


FIG. 3. Parameter space available to the kinetically coupled scalar. Constraints from defect formation [Eq. (3), shaded red] assume production no earlier than $H_* = 10^{-22}$ eV. Nonthermal production occurring when the Hubble rate is near the dark photon’s mass, e.g. via axion or scalar oscillations [17–21], is viable below the dashed red line. The green and blue regions indicate where enhanced DM substructure at k_* [Eq. (17)] could be probed by future astrometric [87] and photometric [88, 89] surveys, respectively. Assuming weak gravity conjectures are true and apply at the displaced field values required by the kinetic coupling, the dashed black line indicates the maximum achievable gauge coupling for which local quantum field theory holds during, e.g., high-scale inflation.

such that early-Universe probes would measure a kinetic mixing different from laboratory ones. Over long enough timescales, laboratory experiments could probe drifts in the kinetic mixing as well.

The success of the scalar production mechanism effectively relies on the Abelian-Higgs theory being extremely weakly coupled at early times, which ostensibly would run afoul of so-called weak gravity conjectures (WGCs) [97]. While the application of the WGC in its various forms to effective field theory and Higgsed gauge symmetries is subtle [98–101], arguments that gravity becomes strongly coupled at a scale $\Lambda_{UV} \sim g_D^{1/3} M_{pl}$ are considered robust [102, 103]. Requiring that gravity remains weakly coupled at the highest energy scale probed by any production scenario therefore places a lower limit on g_D , which, in conjunction with upper bounds from defect formation, can be quite constraining. Requiring the energy scale of inflation to be above Λ_{UV} limits viable inflationary production to $m_{\gamma'} \gtrsim 40$ MeV.

While it is unclear whether WGCs constrain gauge couplings with displaced moduli, were it so they would effectively constrain the initial condition of the scalar field via the combination $\beta\phi_0/f$. Achieving the dark matter relic abundance for a given dark photon mass then requires increasing H_d [via Eq. (20)], diminishing the extent to which the scenario evades defect formation. Combining

the WGC’s lower bound on H_d with the upper bound from defect formation Eq. (3) places an upper bound on the present-day dark gauge coupling. These bounds are set by conditions in the early Universe, i.e., requiring the cutoff scale of quantum gravity to exceed the energy scales of Big Bang Nucleosynthesis, inflation (if measured), or of the SM plasma during dark photon production. Written in terms of the maximum Hubble scale H_{max} , which for BBN is $\sim 10^{-15}$ eV,

$$\frac{g_D}{3 \times 10^{-18}} \lesssim \left(\frac{m_{\gamma'}}{10^{-15} \text{ eV}} \right)^{25/22} \left(\frac{H_{max}}{10^{-15} \text{ eV}} \right)^{-9/22}. \quad (23)$$

Equation (23) takes fiducial values $\beta = 25$ and $\lambda = 1$ (and is not particularly sensitive to either). This bound is weaker than the defect formation bound but would eliminate most (but not all) of the prospective parameter space if the inflationary Hubble scale is $H_{inf} \sim 10^{14}$ GeV [see Fig. 3].

Weak gravity conjectures also motivate ultralight dark photons receiving their mass from the Higgs mechanism rather than the Stückelberg mechanism. In supersymmetry, Stückelberg fields are accompanied by radial degrees of freedom with mass $\sim m_{\gamma'}/g_D$ just like the Higgs, a fact conjectured to hold in any theory of quantum gravity [102]. In this case, inflationary production of dark photons with a Stückelberg mass is just as constrained

as that with a Higgs mass (since the radial modes are produced during inflation if they are too light). It would be worth understanding whether the radial mode plays an important role in other production mechanisms as well.

Though dark matter's current phenomenological relevance resides only at low energies and late times, identifying its fundamental nature offers myriad opportunities to inform high-energy physics. Understanding the mechanisms underlying its mass and its early-Universe production reshapes the implications of direct detection of dark photons. We explore these implications more broadly in companion work [83], with this letter highlighting a scenario whose nonminimality, aside from enabling direct detection in the laboratory, offers promising and complementary observational signatures. These results also motivate searching for signatures of dark photon dark matter from purely gravitational interactions, especially in the near-fuzzy regime $10^{-22} \text{ eV} \lesssim m_{\gamma'} \lesssim 10^{-15} \text{ eV}$ [104–109] where phenomenology can depend on the spin of dark matter [110–116]. Further investigation of consistent dark photon cosmologies will deepen our understanding of the theoretical motivation for and implications of ultralight dark matter detection.

We thank Peter Adshead, Benoit Assi, Masha Baryakhtar, Adrienne Erickcek, Isabel Garcia Garcia, Anson Hook, Junwu Huang, Justin Kaidi, Justin Khoury, and Mark Trodden for insightful discussions. D.C. and Z.J.W. are supported through the Department of Physics and College of Arts and Science at the University of Washington. This material is partially supported by a grant from the Simons Foundation and the hospitality of the Aspen Center for Physics. This work was completed in part at the Perimeter Institute. Research at Perimeter Institute is supported in part by the Government of Canada through the Department of Innovation, Science and Economic Development Canada and by the Province of Ontario through the Ministry of Colleges and Universities. The dark photon parameter space limits and projections quoted above are compiled in Ref. [117].

✉ davidcyn@uw.edu

✉ zweiner@uw.edu

- [1] G. Bertone, D. Hooper, and J. Silk, Particle dark matter: Evidence, candidates and constraints, *Phys. Rept.* **405**, 279 (2005), arXiv:hep-ph/0404175.
- [2] G. Bertone and D. Hooper, History of dark matter, *Rev. Mod. Phys.* **90**, 045002 (2018), arXiv:1605.04909 [astro-ph.CO].
- [3] M. R. Buckley and A. H. G. Peter, Gravitational probes of dark matter physics, *Phys. Rept.* **761**, 1 (2018), arXiv:1712.06615 [astro-ph.CO].
- [4] C. Beasley, J. J. Heckman, and C. Vafa, GUTs and Exceptional Branes in F-theory - I, *JHEP* **01**, 058, arXiv:0802.3391 [hep-th].
- [5] S. A. Abel, M. D. Goodsell, J. Jaeckel, V. V. Khoze, and A. Ringwald, Kinetic Mixing of the Photon with Hidden U(1)s in String Phenomenology, *JHEP* **07**, 124, arXiv:0803.1449 [hep-ph].
- [6] R. Donagi and M. Wijnholt, Breaking GUT Groups in F-Theory, *Adv. Theor. Math. Phys.* **15**, 1523 (2011), arXiv:0808.2223 [hep-th].
- [7] R. Blumenhagen, V. Braun, T. W. Grimm, and T. Weigand, GUTs in Type IIB Orientifold Compactifications, *Nucl. Phys. B* **815**, 1 (2009), arXiv:0811.2936 [hep-th].
- [8] A. Arvanitaki, S. Dimopoulos, S. Dubovsky, N. Kaloper, and J. March-Russell, String Axiverse, *Phys. Rev. D* **81**, 123530 (2010), arXiv:0905.4720 [hep-th].
- [9] R. Blumenhagen, J. P. Conlon, S. Krippendorf, S. Moster, and F. Quevedo, SUSY Breaking in Local String/F-Theory Models, *JHEP* **09**, 007, arXiv:0906.3297 [hep-th].
- [10] M. Goodsell, J. Jaeckel, J. Redondo, and A. Ringwald, Naturally Light Hidden Photons in LARGE Volume String Compactifications, *JHEP* **11**, 027, arXiv:0909.0515 [hep-ph].
- [11] M. Bullimore, J. P. Conlon, and L. T. Witkowski, Kinetic mixing of U(1)s for local string models, *JHEP* **11**, 142, arXiv:1009.2380 [hep-th].
- [12] P. W. Graham, J. Mardon, and S. Rajendran, Vector Dark Matter from Inflationary Fluctuations, *Phys. Rev. D* **93**, 103520 (2016), arXiv:1504.02102 [hep-ph].
- [13] Y. Ema, K. Nakayama, and Y. Tang, Production of purely gravitational dark matter: the case of fermion and vector boson, *JHEP* **07**, 060, arXiv:1903.10973 [hep-ph].
- [14] A. Ahmed, B. Grzadkowski, and A. Socha, Gravitational production of vector dark matter, *JHEP* **08**, 059, arXiv:2005.01766 [hep-ph].
- [15] E. W. Kolb and A. J. Long, Completely dark photons from gravitational particle production during the inflationary era, *JHEP* **03**, 283, arXiv:2009.03828 [astro-ph.CO].
- [16] Y. Nakai, R. Namba, and Z. Wang, Light Dark Photon Dark Matter from Inflation, *JHEP* **12**, 170, arXiv:2004.10743 [hep-ph].
- [17] P. Agrawal, N. Kitajima, M. Reece, T. Sekiguchi, and F. Takahashi, Relic Abundance of Dark Photon Dark Matter, *Phys. Lett. B* **801**, 135136 (2020), arXiv:1810.07188 [hep-ph].
- [18] M. Bastero-Gil, J. Santiago, L. Ubaldi, and R. Vega-Morales, Vector dark matter production at the end of inflation, *JCAP* **04**, 015, arXiv:1810.07208 [hep-ph].
- [19] R. T. Co, A. Pierce, Z. Zhang, and Y. Zhao, Dark Photon Dark Matter Produced by Axion Oscillations, *Phys. Rev. D* **99**, 075002 (2019), arXiv:1810.07196 [hep-ph].
- [20] J. A. Dror, K. Harigaya, and V. Narayan, Parametric Resonance Production of Ultralight Vector Dark Matter, *Phys. Rev. D* **99**, 035036 (2019), arXiv:1810.07195 [hep-ph].
- [21] P. Adshead, K. D. Lozanov, and Z. J. Weiner, Dark photon dark matter from an oscillating dilaton, *Phys. Rev. D* **107**, 083519 (2023), arXiv:2301.07718 [hep-ph].
- [22] P. Arias, D. Cadamuro, M. Goodsell, J. Jaeckel, J. Redondo, and A. Ringwald, WISPy Cold Dark Matter, *JCAP* **06**, 013, arXiv:1201.5902 [hep-ph].
- [23] S. D. McDermott and S. J. Witte, Cosmological evolution of light dark photon dark matter, *Phys. Rev. D* **101**, 063030 (2020), arXiv:1911.05086 [hep-ph].

- [24] A. Caputo, H. Liu, S. Mishra-Sharma, and J. T. Ruder-
man, Modeling Dark Photon Oscillations in Our Inho-
mogeneous Universe, *Phys. Rev. D* **102**, 103533 (2020),
[arXiv:2004.06733 \[astro-ph.CO\]](#).
- [25] A. Caputo, H. Liu, S. Mishra-Sharma, and J. T. Ru-
derman, Dark Photon Oscillations in Our Inhomoge-
neous Universe, *Phys. Rev. Lett.* **125**, 221303 (2020),
[arXiv:2002.05165 \[astro-ph.CO\]](#).
- [26] S. J. Witte, S. Rosauro-Alcaraz, S. D. McDermott, and
V. Poulin, Dark photon dark matter in the presence of in-
homogeneous structure, *JHEP* **06**, 132, [arXiv:2003.13698
\[astro-ph.CO\]](#).
- [27] W. E. East and J. Huang, Dark photon vortex formation
and dynamics, *JHEP* **12**, 089, [arXiv:2206.12432 \[hep-ph\]](#).
- [28] J. Redondo, Helioscope Bounds on Hidden Sector Pho-
tons, *JCAP* **07**, 008, [arXiv:0801.1527 \[hep-ph\]](#).
- [29] H.-S. Zechlin, D. Horns, and J. Redondo, New Con-
straints on Hidden Photons using Very High Energy
Gamma-Rays from the Crab Nebula, *AIP Conf. Proc.*
1085, 727 (2009), [arXiv:0810.5501 \[astro-ph\]](#).
- [30] S. Dubovsky and G. Hernández-Chifflet, Heating up
the Galaxy with Hidden Photons, *JCAP* **12**, 054,
[arXiv:1509.00039 \[hep-ph\]](#).
- [31] N. Vinyoles, A. Serenelli, F. L. Villante, S. Basu, J. Re-
dondo, and J. Isern, New axion and hidden photon con-
straints from a solar data global fit, *JCAP* **10**, 015,
[arXiv:1501.01639 \[astro-ph.SR\]](#).
- [32] M. Baryakhtar, R. Lasenby, and M. Teo, Black Hole
Superradiance Signatures of Ultralight Vectors, *Phys.*
Rev. D **96**, 035019 (2017), [arXiv:1704.05081 \[hep-ph\]](#).
- [33] D. K. Hong, C. S. Shin, and S. Yun, Cooling of young
neutron stars and dark gauge bosons, *Phys. Rev. D* **103**,
123031 (2021), [arXiv:2012.05427 \[hep-ph\]](#).
- [34] D. Wadekar and G. R. Farrar, Gas-rich dwarf galax-
ies as a new probe of dark matter interactions with
ordinary matter, *Phys. Rev. D* **103**, 123028 (2021),
[arXiv:1903.12190 \[hep-ph\]](#).
- [35] X.-J. Bi, Y. Gao, J. Guo, N. Houston, T. Li, F. Xu,
and X. Zhang, Axion and dark photon limits from Crab
Nebula high energy gamma-rays, *Phys. Rev. D* **103**,
043018 (2021), [arXiv:2002.01796 \[astro-ph.HE\]](#).
- [36] M. A. Fedderke, P. W. Graham, D. F. J. Kimball, and
S. Kalia, Earth as a transducer for dark-photon dark-
matter detection, *Phys. Rev. D* **104**, 075023 (2021),
[arXiv:2106.00022 \[hep-ph\]](#).
- [37] W. E. East, Vortex String Formation in Black Hole Su-
perradiance of a Dark Photon with the Higgs Mechanism,
Phys. Rev. Lett. **129**, 141103 (2022), [arXiv:2205.03417
\[hep-ph\]](#).
- [38] S.-P. Li and X.-J. Xu, Production rates of dark photons
and Z' in the Sun and stellar cooling bounds, *JCAP* **09**,
009, [arXiv:2304.12907 \[hep-ph\]](#).
- [39] M. A. Amin, A. J. Long, and E. D. Schiappacasse, Pho-
tons from dark photon solitons via parametric resonance,
JCAP **05**, 015, [arXiv:2301.11470 \[hep-ph\]](#).
- [40] K. Ehret *et al.*, New ALPS Results on Hidden-
Sector Lightweights, *Phys. Lett. B* **689**, 149 (2010),
[arXiv:1004.1313 \[hep-ex\]](#).
- [41] J. Jaeckel and S. Roy, Spectroscopy as a test of
Coulomb's law: A Probe of the hidden sector, *Phys.*
Rev. D **82**, 125020 (2010), [arXiv:1008.3536 \[hep-ph\]](#).
- [42] R. Povey, J. Hartnett, and M. Tobar, Microwave cavity
light shining through a wall optimization and experiment,
Phys. Rev. D **82**, 052003 (2010), [arXiv:1003.0964 \[hep-
ex\]](#).
- [43] R. Bähre *et al.*, Any light particle search II —Techni-
cal Design Report, *JINST* **8**, T09001, [arXiv:1302.5647
\[physics.ins-det\]](#).
- [44] M. Betz, F. Caspers, M. Gasior, M. Thumm, and S. W.
Rieger, First results of the CERN Resonant Weakly
Interacting sub-eV Particle Search (CROWS), *Phys. Rev.*
D **88**, 075014 (2013), [arXiv:1310.8098 \[physics.ins-det\]](#).
- [45] T. Inada, T. Namba, S. Asai, T. Kobayashi, Y. Tanaka,
K. Tamasaku, K. Sawada, and T. Ishikawa, Results of
a Search for Paraphotons with Intense X-ray Beams at
SPring-8, *Phys. Lett. B* **722**, 301 (2013), [arXiv:1301.6557
\[physics.ins-det\]](#).
- [46] S. R. Parker, J. G. Hartnett, R. G. Povey, and M. E.
Tobar, Cryogenic resonant microwave cavity searches for
hidden sector photons, *Phys. Rev. D* **88**, 112004 (2013),
[arXiv:1410.5244 \[hep-ex\]](#).
- [47] M. Schwarz, E.-A. Knabbe, A. Lindner, J. Redondo,
A. Ringwald, M. Schneide, J. Susol, and G. Wiedemann,
Results from the Solar Hidden Photon Search (SHIPS),
JCAP **08**, 011, [arXiv:1502.04490 \[hep-ph\]](#).
- [48] P. Arias, C. Diaz, M. A. Diaz, J. Jaeckel, B. Koch,
and J. Redondo, Hidden Photons in Aharonov-Bohm-
Type Experiments, *Phys. Rev. D* **94**, 015017 (2016),
[arXiv:1603.01282 \[hep-ph\]](#).
- [49] D. Kroff and P. C. Malta, Constraining hidden pho-
tons via atomic force microscope measurements and the
Plimpton-Lawton experiment, *Phys. Rev. D* **102**, 095015
(2020), [arXiv:2008.02209 \[hep-ph\]](#).
- [50] A. Romanenko *et al.*, Search for Dark Photons with
Superconducting Radio Frequency Cavities, *Phys. Rev.*
Lett. **130**, 261801 (2023), [arXiv:2301.11512 \[hep-ex\]](#).
- [51] J. Suzuki, T. Horie, Y. Inoue, and M. Minowa, Ex-
perimental Search for Hidden Photon CDM in the
eV mass range with a Dish Antenna, *JCAP* **09**, 042,
[arXiv:1504.00118 \[hep-ex\]](#).
- [52] S. Knirck, T. Yamazaki, Y. Okesaku, S. Asai, T. Idehara,
and T. Inada, First results from a hidden photon dark
matter search in the meV sector using a plane-parabolic
mirror system, *JCAP* **11**, 031, [arXiv:1806.05120 \[hep-ex\]](#).
- [53] P. Brun, L. Chevalier, and C. Flouzat, Direct Searches
for Hidden-Photon Dark Matter with the SHUKET
Experiment, *Phys. Rev. Lett.* **122**, 201801 (2019),
[arXiv:1905.05579 \[hep-ex\]](#).
- [54] Y. Hochberg, I. Charaev, S.-W. Nam, V. Verma,
M. Colangelo, and K. K. Berggren, Detecting Sub-GeV
Dark Matter with Superconducting Nanowires, *Phys.*
Rev. Lett. **123**, 151802 (2019), [arXiv:1903.05101 \[hep-
ph\]](#).
- [55] L. H. Nguyen, A. Lobanov, and D. Horns, First
results from the WISPDMS radio frequency cavity
searches for hidden photon dark matter, *JCAP* **10**, 014,
[arXiv:1907.12449 \[hep-ex\]](#).
- [56] A. Phipps *et al.*, Exclusion Limits on Hidden-Photon
Dark Matter near 2 neV from a Fixed-Frequency Super-
conducting Lumped-Element Resonator, *Springer Proc.*
Phys. **245**, 139 (2020), [arXiv:1906.08814 \[astro-ph.CO\]](#).
- [57] T. Aralis *et al.* (SuperCDMS), Constraints on dark
photons and axionlike particles from the Super-
CDMS Soudan experiment, *Phys. Rev. D* **101**, 052008
(2020), [Erratum: *Phys.Rev.D* 103, 039901 (2021)],
[arXiv:1911.11905 \[hep-ex\]](#).
- [58] E. Aprile *et al.* (XENON), Light Dark Matter Search
with Ionization Signals in XENON1T, *Phys. Rev. Lett.*

- 123**, 251801 (2019), [arXiv:1907.11485 \[hep-ex\]](#).
- [59] H. An, M. Pospelov, J. Pradler, and A. Ritz, New limits on dark photons from solar emission and keV scale dark matter, *Phys. Rev. D* **102**, 115022 (2020), [arXiv:2006.13929 \[hep-ph\]](#).
- [60] A. V. Dixit, S. Chakram, K. He, A. Agrawal, R. K. Naik, D. I. Schuster, and A. Chou, Searching for Dark Matter with a Superconducting Qubit, *Phys. Rev. Lett.* **126**, 141302 (2021), [arXiv:2008.12231 \[hep-ex\]](#).
- [61] A. Andrianaivalomahefa *et al.* (FUNK Experiment), Limits from the Funk Experiment on the Mixing Strength of Hidden-Photon Dark Matter in the Visible and Near-Ultraviolet Wavelength Range, *Phys. Rev. D* **102**, 042001 (2020), [arXiv:2003.13144 \[astro-ph.CO\]](#).
- [62] L. Barak *et al.* (SENSEI), SENSEI: Direct-Detection Results on sub-GeV Dark Matter from a New Skipper-CCD, *Phys. Rev. Lett.* **125**, 171802 (2020), [arXiv:2004.11378 \[astro-ph.CO\]](#).
- [63] N. Tomita, S. Oguri, Y. Inoue, M. Minowa, T. Nagasaki, J. Suzuki, and O. Tajima, Search for hidden-photon cold dark matter using a K-band cryogenic receiver, *JCAP* **09**, 012, [arXiv:2006.02828 \[hep-ex\]](#).
- [64] E. Aprile *et al.* (XENON), Excess electronic recoil events in XENON1T, *Phys. Rev. D* **102**, 072004 (2020), [arXiv:2006.09721 \[hep-ex\]](#).
- [65] J. Chiles *et al.*, New Constraints on Dark Photon Dark Matter with Superconducting Nanowire Detectors in an Optical Haloscope, *Phys. Rev. Lett.* **128**, 231802 (2022), [arXiv:2110.01582 \[hep-ex\]](#).
- [66] M. A. Fedderke, P. W. Graham, D. F. Jackson Kimball, and S. Kalia, Search for dark-photon dark matter in the SuperMAG geomagnetic field dataset, *Phys. Rev. D* **104**, 095032 (2021), [arXiv:2108.08852 \[hep-ph\]](#).
- [67] L. Manenti *et al.*, Search for dark photons using a multi-layer dielectric haloscope equipped with a single-photon avalanche diode, *Phys. Rev. D* **105**, 052010 (2022), [arXiv:2110.10497 \[hep-ex\]](#).
- [68] H. An, S. Ge, W.-Q. Guo, X. Huang, J. Liu, and Z. Lu, Direct Detection of Dark Photon Dark Matter Using Radio Telescopes, *Phys. Rev. Lett.* **130**, 181001 (2023), [arXiv:2207.05767 \[hep-ph\]](#).
- [69] R. Cervantes *et al.*, Search for 70 μeV Dark Photon Dark Matter with a Dielectrically Loaded Multiwavelength Microwave Cavity, *Phys. Rev. Lett.* **129**, 201301 (2022), [arXiv:2204.03818 \[hep-ex\]](#).
- [70] P. Agnes *et al.* (DarkSide), Search for Dark Matter Particle Interactions with Electron Final States with DarkSide-50, *Phys. Rev. Lett.* **130**, 101002 (2023), [arXiv:2207.11968 \[hep-ex\]](#).
- [71] S. Kotaka *et al.* (DOSUE-RR), Search for Dark Photon Dark Matter in the Mass Range 74–110 μeV with a Cryogenic Millimeter-Wave Receiver, *Phys. Rev. Lett.* **130**, 071805 (2023), [arXiv:2205.03679 \[hep-ex\]](#).
- [72] X. Fan, G. Gabrielse, P. W. Graham, R. Harnik, T. G. Myers, H. Ramani, B. A. D. Sukra, S. S. Y. Wong, and Y. Xiao, One-Electron Quantum Cyclotron as a Milli-eV Dark-Photon Detector, *Phys. Rev. Lett.* **129**, 261801 (2022), [arXiv:2208.06519 \[hep-ex\]](#).
- [73] K. Ramanathan, N. Klimovich, R. Basu Thakur, B. H. Eom, H. G. LeDuc, S. Shu, A. D. Beyer, and P. K. Day, Wideband Direct Detection Constraints on Hidden Photon Dark Matter with the QUALIPHIDE Experiment, *Phys. Rev. Lett.* **130**, 231001 (2023), [arXiv:2209.03419 \[astro-ph.CO\]](#).
- [74] F. Bajjali *et al.*, First results from BRASS-p broadband searches for hidden photon dark matter, *JCAP* **08**, 077, [arXiv:2306.05934 \[hep-ex\]](#).
- [75] G. B. Gelmini, A. J. Millar, V. Takhistov, and E. Vitagliano, Probing dark photons with plasma haloscopes, *Phys. Rev. D* **102**, 043003 (2020), [arXiv:2006.06836 \[hep-ph\]](#).
- [76] J. Liu *et al.* (BREAD), Broadband Solenoidal Haloscope for Terahertz Axion Detection, *Phys. Rev. Lett.* **128**, 131801 (2022), [arXiv:2111.12103 \[physics.ins-det\]](#).
- [77] B. Godfrey *et al.*, Search for dark photon dark matter: Dark E field radio pilot experiment, *Phys. Rev. D* **104**, 012013 (2021), [arXiv:2101.02805 \[physics.ins-det\]](#).
- [78] M. Baryakhtar, J. Huang, and R. Lasenby, Axion and hidden photon dark matter detection with multilayer optical haloscopes, *Phys. Rev. D* **98**, 035006 (2018), [arXiv:1803.11455 \[hep-ph\]](#).
- [79] D. S. Akerib *et al.* (LZ), Projected sensitivities of the LUX-ZEPLIN experiment to new physics via low-energy electron recoils, *Phys. Rev. D* **104**, 092009 (2021), [arXiv:2102.11740 \[hep-ex\]](#).
- [80] S. Chaudhuri, P. W. Graham, K. Irwin, J. Mardon, S. Rajendran, and Y. Zhao, Radio for hidden-photon dark matter detection, *Phys. Rev. D* **92**, 075012 (2015), [arXiv:1411.7382 \[hep-ph\]](#).
- [81] B. Holdom, Two $U(1)$'s and Epsilon Charge Shifts, *Phys. Lett. B* **166**, 196 (1986).
- [82] T. G. Rizzo, Kinetic Mixing and Portal Matter Phenomenology, *Phys. Rev. D* **99**, 115024 (2019), [arXiv:1810.07531 \[hep-ph\]](#).
- [83] D. Cyncynates and Z. J. Weiner, (forthcoming).
- [84] T. Damour, F. Piazza, and G. Veneziano, Violations of the equivalence principle in a dilaton runaway scenario, *Phys. Rev. D* **66**, 046007 (2002), [arXiv:hep-th/0205111](#).
- [85] M. Gasperini, F. Piazza, and G. Veneziano, Quintessence as a runaway dilaton, *Phys. Rev. D* **65**, 023508 (2002), [arXiv:gr-qc/0108016](#).
- [86] T. Damour, F. Piazza, and G. Veneziano, Runaway dilaton and equivalence principle violations, *Phys. Rev. Lett.* **89**, 081601 (2002), [arXiv:gr-qc/0204094](#).
- [87] K. Van Tilburg, A.-M. Taki, and N. Weiner, Halometry from Astrometry, *JCAP* **07**, 041, [arXiv:1804.01991 \[astro-ph.CO\]](#).
- [88] A. Arvanitaki, S. Dimopoulos, M. Galanis, L. Lehner, J. O. Thompson, and K. Van Tilburg, Large-misalignment mechanism for the formation of compact axion structures: Signatures from the QCD axion to fuzzy dark matter, *Phys. Rev. D* **101**, 083014 (2020), [arXiv:1909.11665 \[astro-ph.CO\]](#).
- [89] L. Dai and J. Miralda-Escudé, Gravitational Lensing Signatures of Axion Dark Matter Minihalos in Highly Magnified Stars, *Astron. J.* **159**, 49 (2020), [arXiv:1908.01773 \[astro-ph.CO\]](#).
- [90] E. J. Copeland, A. R. Liddle, and D. Wands, Exponential potentials and cosmological scaling solutions, *Phys. Rev. D* **57**, 4686 (1998), [arXiv:gr-qc/9711068](#).
- [91] P. J. Steinhardt, L.-M. Wang, and I. Zlatev, Cosmological tracking solutions, *Phys. Rev. D* **59**, 123504 (1999), [arXiv:astro-ph/9812313](#).
- [92] E. J. Copeland, M. Sami, and S. Tsujikawa, Dynamics of dark energy, *Int. J. Mod. Phys. D* **15**, 1753 (2006), [arXiv:hep-th/0603057](#).
- [93] Z. Hou, R. Keisler, L. Knox, M. Millea, and C. Reichardt, How Massless Neutrinos Affect the Cosmic Microwave

- Background Damping Tail, *Phys. Rev. D* **87**, 083008 (2013), [arXiv:1104.2333 \[astro-ph.CO\]](#).
- [94] S. Bashinsky and U. Seljak, Neutrino perturbations in CMB anisotropy and matter clustering, *Phys. Rev. D* **69**, 083002 (2004), [arXiv:astro-ph/0310198](#).
- [95] D. Baumann, D. Green, J. Meyers, and B. Wallisch, Phases of New Physics in the CMB, *JCAP* **01**, 007, [arXiv:1508.06342 \[astro-ph.CO\]](#).
- [96] N. Blinov, M. J. Dolan, P. Draper, and J. Shelton, Dark Matter Microhalos From Simplified Models, *Phys. Rev. D* **103**, 103514 (2021), [arXiv:2102.05070 \[astro-ph.CO\]](#).
- [97] N. Arkani-Hamed, L. Motl, A. Nicolis, and C. Vafa, The String landscape, black holes and gravity as the weakest force, *JHEP* **06**, 060, [arXiv:hep-th/0601001](#).
- [98] P. Saraswat, Weak gravity conjecture and effective field theory, *Phys. Rev. D* **95**, 025013 (2017), [arXiv:1608.06951 \[hep-th\]](#).
- [99] B. Heidenreich, M. Reece, and T. Rudelius, Evidence for a sublattice weak gravity conjecture, *JHEP* **08**, 025, [arXiv:1606.08437 \[hep-th\]](#).
- [100] B. Heidenreich, M. Reece, and T. Rudelius, The Weak Gravity Conjecture and Emergence from an Ultraviolet Cutoff, *Eur. Phys. J. C* **78**, 337 (2018), [arXiv:1712.01868 \[hep-th\]](#).
- [101] N. Craig and I. Garcia Garcia, Rescuing Massive Photons from the Swampland, *JHEP* **11**, 067, [arXiv:1810.05647 \[hep-th\]](#).
- [102] M. Reece, Photon Masses in the Landscape and the Swampland, *JHEP* **07**, 181, [arXiv:1808.09966 \[hep-th\]](#).
- [103] D. Harlow, B. Heidenreich, M. Reece, and T. Rudelius, Weak gravity conjecture, *Rev. Mod. Phys.* **95**, 035003 (2023), [arXiv:2201.08380 \[hep-th\]](#).
- [104] W. Hu, R. Barkana, and A. Gruzinov, Cold and fuzzy dark matter, *Phys. Rev. Lett.* **85**, 1158 (2000), [arXiv:astro-ph/0003365](#).
- [105] H.-Y. Schive, T. Chiueh, and T. Broadhurst, Cosmic Structure as the Quantum Interference of a Coherent Dark Wave, *Nature Phys.* **10**, 496 (2014), [arXiv:1406.6586 \[astro-ph.GA\]](#).
- [106] L. Hui, J. P. Ostriker, S. Tremaine, and E. Witten, Ultralight scalars as cosmological dark matter, *Phys. Rev. D* **95**, 043541 (2017), [arXiv:1610.08297 \[astro-ph.CO\]](#).
- [107] L. Hui, Wave Dark Matter, *Ann. Rev. Astron. Astrophys.* **59**, 247 (2021), [arXiv:2101.11735 \[astro-ph.CO\]](#).
- [108] N. Dalal and A. Kravtsov, Excluding fuzzy dark matter with sizes and stellar kinematics of ultrafaint dwarf galaxies, *Phys. Rev. D* **106**, 063517 (2022), [arXiv:2203.05750 \[astro-ph.CO\]](#).
- [109] M. A. Amin and M. Mirbabayi, A lower bound on dark matter mass, [arXiv:2211.09775 \[hep-ph\]](#) (2022).
- [110] P. Adshead and K. D. Lozanov, Self-gravitating Vector Dark Matter, *Phys. Rev. D* **103**, 103501 (2021), [arXiv:2101.07265 \[gr-qc\]](#).
- [111] H.-Y. Zhang, M. Jain, and M. A. Amin, Polarized vector oscillons, *Phys. Rev. D* **105**, 096037 (2022), [arXiv:2111.08700 \[astro-ph.CO\]](#).
- [112] M. Jain and M. A. Amin, Polarized solitons in higher-spin wave dark matter, *Phys. Rev. D* **105**, 056019 (2022), [arXiv:2109.04892 \[hep-th\]](#).
- [113] M. Gorghetto, E. Hardy, J. March-Russell, N. Song, and S. M. West, Dark photon stars: formation and role as dark matter substructure, *JCAP* **08** (08), 018, [arXiv:2203.10100 \[hep-ph\]](#).
- [114] M. A. Amin, M. Jain, R. Karur, and P. Mocz, Small-scale structure in vector dark matter, *JCAP* **08** (08), 014, [arXiv:2203.11935 \[astro-ph.CO\]](#).
- [115] M. Jain, M. A. Amin, J. Thomas, and W. Wanichwecharungruang, Kinetic relaxation and Bose-star formation in multicomponent dark matter, *Phys. Rev. D* **108**, 043535 (2023), [arXiv:2304.01985 \[astro-ph.CO\]](#).
- [116] M. Jain, W. Wanichwecharungruang, and J. Thomas, Kinetic relaxation and nucleation of Bose stars in self-interacting wave dark matter, [arXiv:2310.00058 \[astro-ph.CO\]](#) (2023).
- [117] A. Caputo, A. J. Millar, C. A. J. O'Hare, and E. Vitagliano, Dark photon limits: A handbook, *Phys. Rev. D* **104**, 095029 (2021), [arXiv:2105.04565 \[hep-ph\]](#).